2023 EAGE ANNUAL
84TH CONFERENCE & EXHIBITION
VIENNA | AUSTRIA

Dynamic resolution TLFWI for velocity model building beyond the reach of diving waves

M. Wang[1], Y. Xie[1], P. Deng[1], Y. Chen[1], J. Cai[1], X. Li[1]

[1] CGG

Summary

Dynamic Resolution Time-Lag FWI (DR-TLFWI) aims to use both diving waves and reflections for velocity update with optimized low- and high-wavenumber components from shallow to deep section. The proposed method builds contrast into the velocity model, enabling the simulation of reflections. The iterative velocity update scheme of DR-TLFWI handles multiples hence it can work with raw seismic data. The tomographic term of the velocity gradient from the reflection energy (low-wavenumber components) is typically much weaker than other components, due to additional reflections taking place during wave propagation. We propose to compensate these additional reflections by the corresponding illumination volume derived in each iteration of the FWI scheme. As such, a dynamic weighting can be devised for the different components in the FWI kernel to optimize the contributions across low- and high-wavenumber components of the velocity model. We use the time-lag objective function to avoid the dominance of strong amplitudes. Both synthetic and field dataset applications show that DR-TLFWI can reasonably update the velocity models from shallow section to deep beyond the reach of diving waves, especially when input data has a limited offset range. The images are improved accordingly with reduced structural undulations.

Dynamic resolution TLFWI for velocity model building beyond the reach of diving waves

Introduction

Full Waveform Inversion (FWI) uses the full wavefield as input data and therefore can naturally update velocity model with both diving waves and reflection energy. For velocity update beyond diving wave penetration depth, FWI must rely on reflection energy. However, the low-wavenumber velocity updates driven by reflections are often weak compared to the high-wavenumber component which has limited impact on kinematics, thus making it a challenge to use FWI to fully extract the benefit of reflection energy. For this reason, conventional tools, for instance ray-based reflection tomography, are still frequently used for velocity model update beyond the reach of diving waves. Nevertheless, a FWI strategy to better extract the benefit of reflections is of high interest, especially for complex overburden with rapid lateral velocity variations and input data with limited offset ranges.

In the last decade, attempts and developments have been made in industry and academia to address this issue. Those works can be split into two major approaches. One approach involves an intermediate model, either velocity (Irabor et al., 2016) or density (Gomes et al., 2017), to generate the contrast for reflection simulation. Following that, low-wavenumber components can be extracted either by selectively correlating wavefields traveling in different directions (Tang et al., 2013) or via scattering angle filtering (Alkhalifah, 2015). The intermediate model will be reproduced in each iteration as an additional cost compared to the conventional FWI. The other approach is to use Born modelling where seismic images are used as a second source to generate the reflected wavefield; hence it can naturally isolate the low-wavenumber velocity (Xu et al., 2012; Sun et al., 2017; Wang et al., 2018). Upon applications, we observed that those methods typically work better with primary only data which means pre-processing is required. Furthermore, convergence is hard to guarantee due to the incomplete velocity gradient. To better derive the benefits of reflection energy in raw seismic data, a straightforward way has been explored that uses a weighting factor to promote the tomographic term from reflection energies in full wavefield gradient (Tang et al., 2013; Deng et al., 2022).

In this paper, we present a Dynamic Resolution TLFWI (DR-TLFWI) workflow that attempts to exploit the benefit of both diving waves and reflected waves. It builds contrast into velocity models enabling a natural simulation of reflections. It performs a new compensation scheme to account for the impact of reflectivity on velocity gradients. The corresponding dynamic weighting is applied on different components in FWI kernel to optimize the contributions on low- and high-wavenumber parts of the velocity model. The proposed method uses the time-lag cost function proposed by Zhang et al. (2018) to downplay amplitudes for a more robust inversion. In the following sections, we will discuss the methodology of the proposed approach and its application on both synthetic and real data.

Method

Modelling reflections is an important step in making use of reflection energy for velocity update. Gomes et al. (2018) have shown that using LSRTM image as reflectivity has given a better tomography update compared with using RTM image because of the accuracy of reflectivity. For generating the reflections, we propose to use the iteratively updated velocity with migration term, or effectively the FWI Image (Zhang et al., 2020), considering that FWI Imaging often gives superior image quality to RTM or LSRTM due to the use of full wavefield. In addition, this workflow can also benefit from the use of raw data whilst RTM- or LSRTM-based reflectivity requires pre-processed primary only data as input. The simplified processing flow greatly cuts down the turnaround of processing.

Reflection data produce two components of the FWI gradient: the high-wavenumber component, or the migration term; and the low-wavenumber component, also known as the tomographic term or “rabbit ears”. In conventional FWI, the velocity update beyond the diving wave penetration is overwhelmed by high-wavenumber components which have less impact on the kinematics. Therefore, being able to use the low-wavenumber velocity update is another important step. Deng et al. (2022) used a weighting factor to promote the tomographic term and to solve the fault shadow problem. The weighting was

derived on a trial-and-error basis which was suitable to address the fault shadow problem encountered in their data; however, it may not work in general. Approximated Hessian can be another way for applying adaptive scalar to promote tomographic term (Tang et al., 2013). The root cause of weaker tomographic term compared to the migration term is the additional reflection taking place during wave propagation. FWI gradient can always be represented as a cross-correlation between the source and receiver wavefields regardless of the objective function (Tang et al. 2013). We can organize it as below,

$$G_m = \int_{t=0}^{tmax} \big(S(m) * R(m) + \delta S(m) * R(m) + S(m) * \delta R(m)\big) dt \quad (1)$$

with the gradient split into three parts. The first term is related to the diving wave contribution and the migration term, whilst the last two relate to the tomographic term from reflections. S and R represent the source and receiver side wavefields respectively, while δS and δR are the scattered wavefields. The energy of the scattered wavefield is usually at least one magnitude lower than the transmitted one. Without illumination compensation, we can imagine the weak energy contribution of tomographic term in the total velocity gradient. We propose applying a dynamic weighting, which is iteration variant, onto the different components of gradient after separation, allowing compensation for the energy lost on tomographic term due to additional reflection process. Indeed, the shallow section typically has good low- and high-wavenumber components from diving waves and reflections; therefore, we keep the original gradient intact by using a pre-estimated mask. Only in the zone dominated by reflections will the tomographic term be promoted and recombined into the full gradient during inversion to make better use of the contribution from the full wavefield. Through an iterative process, the tomographic term will be accumulated from low to higher frequency and the resolution will be improved accordingly. The time-lag cost function (Zhang et al., 2018) is used in this proposed method to mitigate the negative impact from the amplitude discrepancy between the real and modelled data.

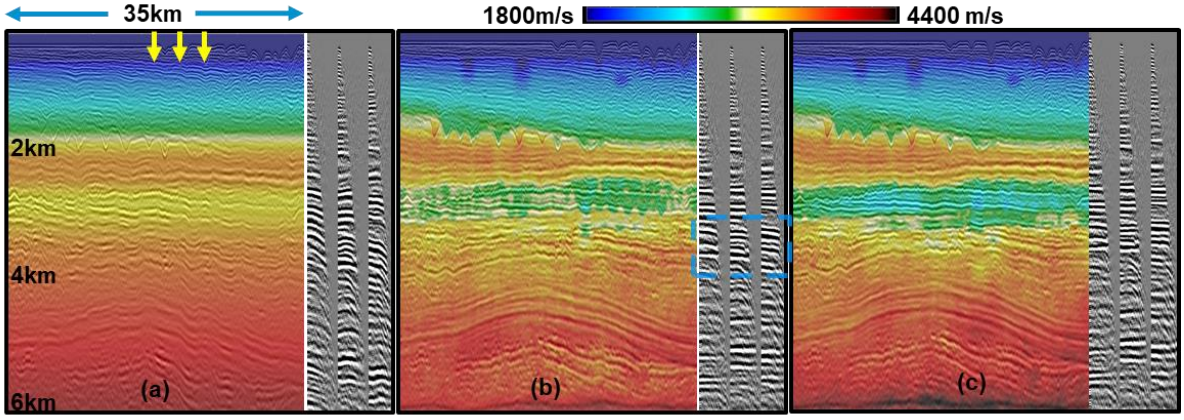

Figure 1 *Velocity overlaid on PSDM stack and selected CIGs with the location indicated by yellow arrows from (a) initial velocity, (b) TLFWI inverted velocity and (c) DR-TLFWI inverted velocity.*

Synthetic example

Chevron 2014 synthetic data is a good benchmark for checking the capability of low-wavenumber velocity update with reflections in FWI framework. The starting velocity is basically 1D but with water velocity honoured, as shown in Figure 1(a). The distortion on pre-stack depth migration (PSDM) stack and visible moveout on common image gathers (CIGs) indicate the velocity is far from true. Using both diving waves and reflections, we run through TLFWI from 3 to 12Hz, and the corresponding results are shown in Figure 1 (b). We can see the shallow velocity is well resolved by diving waves, and the slow velocity anomalies and shallow channels are captured. However, we observe residual curvature below 2 km which is corresponding to a slow velocity layer just beneath the penetration depth of diving waves. In principle, TLFWI is able to correct some low-wavenumber velocity errors beyond the reach of diving wave due to TLFWI velocity gradient containing tomographic component from reflections. However, the magnitude is small, so the correction is minimum. Using DR-TLFWI from the same starting model, the low-wavenumber component from reflections has been promoted and can better correct the velocity error in the deep section as shown in Figure 1 (c). Overall, the slow velocity layer has been well

resolved, reflectors have become better focused, and gathers are mostly flat. When the starting velocity is not that far from true, we would not expect such a big difference between TLFWI and DR-TLFWI.

Field data examples

The proposed method has been applied on field dataset with promising results. The first example is OBN data from offshore China. The maximum offset is 16 km; however, the diving wave penetrates only down to 2.2 km due to the high velocity layer around 1.5-2.2 km. DR-TLFWI is used after both TLFWI and conventional ray-based reflection tomography are applied. Figure 2 (a) shows the velocity overlayed on its image before DR-TLFWI. The line cuts through the target area and illustrates the presence of a large gas body in the deep section. Despite the efforts with conventional tools, there are still some residual distortions in the image as highlighted in the zoomed-in PSDM section in Figure 2 (c). With DR-TLFWI, velocity has been fine-tuned, especially at the complex gas body as shown in Figure 2 (b). Unreasonable bumps on reflectors have been reduced with the DR-TLFWI inverted velocity as shown in Figure 2 (d). Though the update seems subtle, it may be vital for reservoir studies.

The second example is NAZ streamer data from NWS, Australia. The maximum cable length is 5.5 km and diving waves only reach to about 1 km below the seabed. The survey has several phases of paleo-channelling with varied infill. The starting velocity in Figure 3 (a) has a reasonable background velocity but limited lateral variation. The corresponding image in Figure 3 (b) shows the undulations on the reflectors beneath those complex structures, highlighted in the zoomed-in section in Figure 3 (c). DR-TLFWI captures the complex velocity variations in the overburden, hereby greatly reducing the structure undulations in the final image displayed in Figures 3 (e) and (f). The velocity, shown in Figure 3 (d), reveals the fine details of the structures which may help with geologic interpretation.

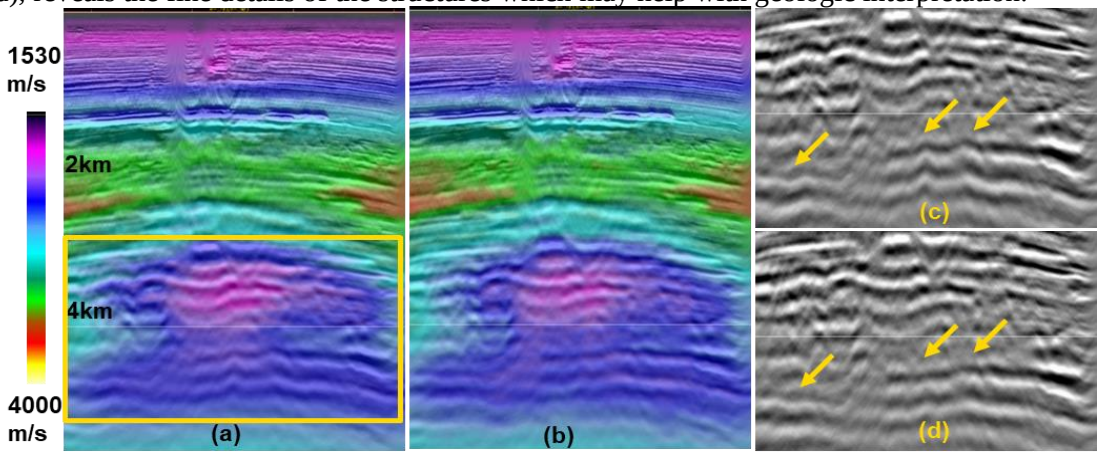

Figure 2 *(a) Input velocity for DR-TLFWI overlayed on PSDM stack, (b) DR-TLFWI updated velocity overlayed on PSDM stack; and their zoomed-in PSDM sections in (c) and (d).*

Discussions and Conclusions

We propose DR-TLFWI to better update velocity from shallow to deep section beyond the reach of diving waves. The method uses iteratively updated velocity for natural simulation of reflections and applies a dynamic weighting onto different components of gradient to compensate for the effect of reflection on the tomographic term. The varied examples validate the effectiveness of this approach for velocity update using raw seismic data. However, some limitations remain. Wang et al. (2018) have discussed the ambiguity between velocity and depth of reflectors when reflections are used in FWI. Thanks to the wave decomposition technique, the migration term contaminated with the error from the initial velocity can always be taken out from the velocity after we have updated the low-wavenumber component. A new migration term can be built up in a new cycle of FWI and the reflector will be improved in terms of depth accuracy. Therefore, the ambiguity is reduced. Low vertical resolution is another challenge for reflections in FWI which has been discussed by Gomes et al. (2017). The velocity update from tomographic term by reflections typically appears stripy compared with the update from

the diving waves. The strategy of using the time-lag cost objective function helps to reduce the bias of strong reflections; however, low vertical resolution is still the fundamental issue for reflections in FWI. It may be even worse for narrow azimuth streamer data because of the incompleteness of reflection energy. Optimized acquisition would be required to address complex structures with higher fidelity.

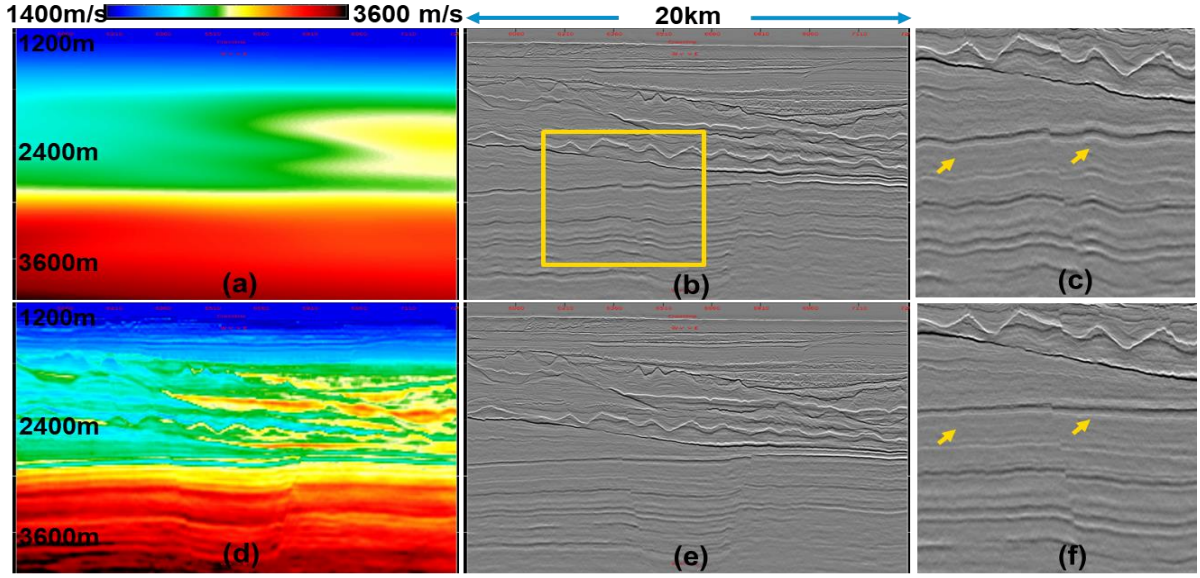

Figure 3 *Velocity, PSDM stack and zoomed-in section at rectangle zone, from (a~c) initial velocity, (d~f) DR-TLFWI inverted velocity.*

Acknowledgements

The authors thank CGG and CNOOC for permission to publish this paper.

References

Alkhalifah, T. [2015]. Scattering-angle based filtering of the waveform inversion gradients. *Geophysical Journal International*, 200(1), 363–373.

Deng, P., Lee, Y., Wang, M., Li, J., Hung, B., Lee, K., Kim, M., Kim, S., Jeong, C., Li, M. and He, J. [2022]. Correction fault shadows – a case study comparison of fault-constrained tomography and time-lag full-waveform inversion. *83rd EAGE Annual International Meeting*, Expanded Abstracts, 1-5.

Gomes, A. and Chazalnoel, N. [2017]. Extending the reach of FWI with reflection data: Potential and challenges. *87th SEG Annual International Meeting*, Expanded Abstracts, 1454-1459.

Gomes, A. and Yang, Z. [2018]. Improving reflection FWI reflectivity using LSRTM in the curvelet domain. *88th SEG Annual International Meeting*, Expanded Abstracts, 1248-1252.

Irabor, K. and Warner, M. [2016]. Reflection FWI. *86th SEG Annual International Meeting*, Expanded Abstracts, 1136-1140.

Sun, D., Jiao, K., Xu, C., Zhang, L. and Vigh, D. [2017]. Born modelling based adjustive reflection full waveform inversion. *87th SEG Annual International Meeting*, Expanded Abstracts, 1460-1465.

Tang, Y., Lee, S., Baumstein, A. and Hinkley, D. [2013]. Tomographically enhanced full wavefield inversion. *83rd SEG Annual International Meeting*, Expanded Abstracts, 1037-1041.

Wang, P., Zhang, Z., Wei, Z. and Huang, R. [2018]. A demigration-based reflection full-waveform inversion workflow. *88th SEG Annual International Meeting*, Expanded Abstracts, 1138-1142.

Xu, S., Wang, D., Chen, F., Lambare, G. and Zhang, Y. [2012]. Inversion on reflected seismic wave. *82nd SEG Annual International Meeting*, Expanded Abstracts, 1–7.

Zhang, Z., Mei, J., Lin, F., Huang, R. and Wang, P. [2018]. Correcting for salt misinterpretation with full-waveform inversion. *88th SEG Annual International Meeting*, Expanded Abstracts, 1143-1147.

Zhang, Z., Wu, Z., Wei, Z., Mei, J., Huang, R. and Wang, P. [2020]. FWI Imaging: Full-wavefield imaging through full-waveform inversion. *90th SEG Annual International Meeting*, Expanded Abstracts, 656-660.